Leader-Follower Dynamics for Diffusion-based Molecular Communication

Jorge Torres Gómez*, Wayan Wicke†, Karel Toledo‡, Robert Schober†, and Falko Dressler*

*School of Electrical Engineering and Computer Science, TU Berlin, Berlin, Germany
†Institute for Digital Communications, University of Erlangen-Nuremberg, Erlangen, Germany
‡Department of Electronics, Federico Santa María Technical University, Valparaiso, Chile

Abstract—Nanomachines are envisioned for a variety of applications in the industry and health sectors operating as sensors and actuators. Considering their potential mobility, it is relevant to study the capability of nanomachines to cooperate in molecular communication scenarios. To this end, we provide new insights into the leader-follower dynamics when a mobile leader node moves randomly in three-dimensional space and emits molecules into a diffusive environment to send information about its position to a follower node. In this paper, we investigate the random distance between the two nodes due to decision errors at the follower and analyze an upper bound for the average distance as a function of time. Simulations are provided to validate our analytical results. Moreover, by comparing to the benchmark scenario of uncoordinated movement of leader and follower, we investigate for which parameters the follower can reliably follow the leader.

I. INTRODUCTION

Recently, the use of nanomachines has become a focus of attention with a variety of applications within future generations of wireless networks [1] and health care systems [2]. Advances in synthetic biology allow for the realization of communication components [3], thus, enabling nanonetwork infrastructures. Furthermore, the dynamic capabilities of nano-sized nodes enable the controlled mobility of nanonetworks boosting applications in industrial environments like detection of corrosion, or damages in pipes, and their repairing as well [4]. In biomedical applications, these mobile nanonetworks are expected to locate and monitor targets that can dynamically appear, move, or disappear like pathogens, infectious microorganisms, chemical compounds, or cancer cells in the human circulatory system [5].

In mobile nanonetworks, it is crucial that nanomachines exchange information to coordinate as a group. However, the inherently dynamic environment results in variable channel conditions. The channel variability impacts the communication performance impeding their ability to communicate and coordinate their operations. These aspects have been theoretically addressed through deriving the time-varying channel impulse response [6] and related metrics such as the received signal strength [7].

These theoretical results provide the basis for optimizing design parameters for specific mobile molecular communication schemes, including the design of an optimized threshold [8], and evaluating the system performance in terms of the bit error rate [9] and achievable rate [10]. Also, transmission with a differential encoding [11] or by using different types of molecules [12] has been investigated and reception has been proposed exploiting multiple measurements over time [13] or using adaptive signal detection techniques [14]. These solutions for point-to-point connections facilitate cooperation among mobile nanomachines. Moreover, using different types of molecules, communication strategies have been devised for efficient spreading of several mobile nodes and to lead them to fixed [15], [16] and moving [5], [17] targets, and potentially incorporating relay nodes to extend the communication range [18]. Tracking the target node, also referred to as the leader in the following, can be realized through a variety of mechanisms regarding the communication of the leader node's position to the follower node. For instance, the follower node may track the diffusing molecules of the leader node through their gradient [15], [16], or the leader node may encode its current position and send it via diffusion to the follower node via a specific modulation technique [19].

For proper cooperation between the nanodevices, the distance between the leader and follower needs to be kept small, which is difficult since distortions arise from the random time-varying channel, noise, and interference. Moreover, estimation errors at the follower increase the distance between leader and follower which in turn impacts the estimation errors such that the follower can get lost. Since, studying the distance between leader and follower over time has only been studied through simulations so far, in the following, we want to consider a simple leader-follower system where the leader is mobile and sends time-periodic position updates to the follower. To this end, we propose a low-complexity leader-follower communication scheme where the leader and follower move in discrete spatial steps and information on the position of the leader is encoded in the performed jumps of the leader node. Moreover, considering the randomness of the leader node's position, we derive an upper bound for the average distance between leader and follower, as a function of time, and validate our results by simulations.

This paper is structured as follows. The leader-follower system model is introduced in Section II. Tracking of the leader by the follower is analyzed in Section III, and numerical results are provided in Section IV. Finally, Section V concludes this paper.
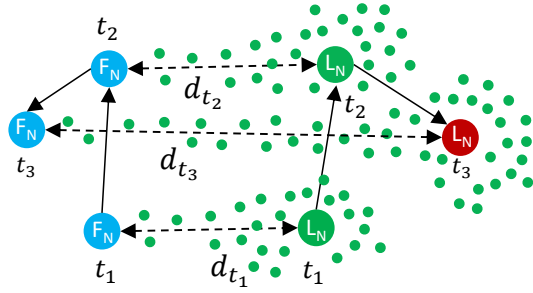
Fig. 1. Illustration of the time varying position of the leader node and the varying distance.
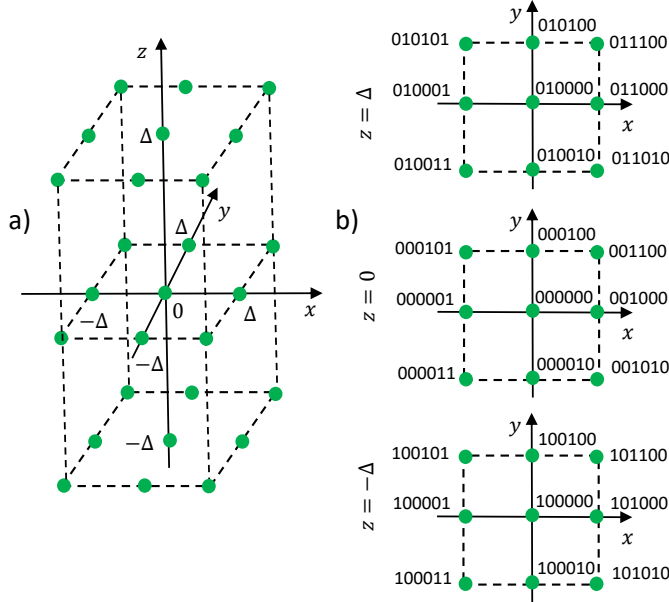

Fig. 2. Constellation to encode the leader's positions. a) Total of quantified jumps. b) Binary code for the quantified jumps.

II. SYSTEM MODEL

In this section, we introduce the leader-follower scenario and provide the underlying signal model.

A. Leader-Follower Scenario

We consider the scenario in Fig. 1, where for three time instances t_1, t_2, and t_3 the position of the leader, denoted by L_N, and of the follower, denoted by F_N is sketched. The position of leader and follower are denoted by $\mathbf{p}_L(t) = [x(t), y(t), z(t)]$ and $\mathbf{p}_F(t)$, respectively. The distances between leader and follower, corresponding to these time instances, are denoted by d_{t_1}, d_{t_2}, and d_{t_3}, respectively. It is assumed that at time t_1, the leader starts transmitting to the follower the next position increment $\mathbf{p}_L(t_2) - \mathbf{p}_L(t_1)$. After transmission and reception of the information representing this position increment, leader and follower move to the actual and estimated position, respectively. In this way, without detection errors, the distance between leader and follower would be constant over time.

After communicating the next position increment at time t_{i-1} to the follower, the leader updates its current position for time t_i as follows.

$$\mathbf{p}_L(t_i) = \mathbf{p}_L(t_{i-1}) + \boldsymbol{\Delta}_L, \qquad (1)$$

where $\boldsymbol{\Delta}_L = [\Delta_x, \Delta_y, \Delta_z]$ is the step vector with position increments Δ_x, Δ_y, and Δ_z, randomly chosen from a uniform distribution in the set $\{-\Delta, 0, \Delta\}$. Vector $\boldsymbol{\Delta}_L$ is also referred to as jump in the following and can take on any of the coordinates represented in Fig. 2 a). In other words, we assume a discrete spatial grid with distance Δ between two neighboring points and movement with no preferred direction of the leader. Moreover, we assume that the step size Δ is chosen as [2]

$$\Delta = \sqrt{2 D_{T_x} \Delta t}, \qquad (2)$$

where D_{T_x} is a diffusion coefficient modeling the dynamics of the transmitter movement and Δt is the discrete-time step. This discrete-time step is assumed to represent the time duration for the leader movement, as well as for transmitting its position increment, the duration of which the leader stays at the same position. Then, for the time instances defined above we have $t_i = t_{i-1} + 2\Delta t$, i.e., during time t_{i-1} and time $t_{i-1} + \Delta t$ the leader stays at position $\mathbf{p}_L(t_{i-1})$ and transmits its position increment to the follower and then during time $t_{i-1} + \Delta t$ and time $t_{i-1} + 2\Delta t$, the leader moves to the next position $\mathbf{p}_L(t_i)$.

After detection of the information representing the position increment at time $t_{i-1} + \Delta t$, the follower will move time-synchronous with the leader in the estimated direction $\boldsymbol{\Delta}_{\mathbf{R_x}}$ and update its position accordingly as

$$\mathbf{p}_F(t_i) = \mathbf{p}_F(t_{i-1}) + \boldsymbol{\Delta}_{\mathbf{R_x}}. \qquad (3)$$

Communication between leader and follower works as follows. The jump vector $\boldsymbol{\Delta}_L$, is encoded in a 6-bit sequence, as depicted in Fig. 2 b, where a Gray mapping [20] is applied to reduce the impact of decoding errors, i.e., the encoding of neighboring constellation points differs in one bit only. Considering the fixed time step Δt of the leader movement, the resulting bit duration is given by $T_b = \frac{\Delta t}{6}$. For modulation, the leader employs on-off keying to send the 6-bit sequence representing the jump to the follower. In this way, a total of N_{T_x} molecules will be released into the environment when transmitting a one, and no emission will be made when transmitting a zero. Once released at $\tau = jT_b$, the molecules will diffuse with a diffusion coefficient D, and some will arrive at the follower node. For each bit, the leader will wait for the time duration of T_b before transmitting the next one and also before moving to the next position.

For signal reception, the follower is modeled as a transparent sphere with volume $V_{R_x} = \frac{4}{3}\pi r^3$, where r is the radius of the sphere. We assume that the receiver is able to sample synchronously the received signal at the peak time of the channel impulse response, denoted by T_{d_τ}. This may be accomplished when the receiver samples the incoming signal with a sufficient rate to distinguish the peak, which may

require some additional signal processing. Samples are taken at times $t_j = t_{i-1} + (j-1)T_b + T_{d_\tau}$ for bits $j = 1, 2, 3, 4, 5, 6$ which we denote as $N_{R_x}(j)$. Thereby, we assume that the bit duration T_b is larger than the peak time of the channel impulse response given by

$$T_{d_\tau} = \frac{d_\tau^2}{6D}, \tag{4}$$

where d_τ is the distance between leader and follower.

We assume that communication is impaired by the time-variant channel resulting from the movement of both nodes, including intersymbol interference (ISI) within each 6-bit sequence, and by a background noise of strength λ_0 characterizing the number of interfering noise molecules per unit time [21]. Then, bit j is detected as a '1' when $N_{R_x}(t_j) > N_h$ and as a '0' otherwise.

Finally, from the detected 6-bit sequence the detected jump is decoded as the nearest neighbor among the available codewords (see Fig. 2 b).

B. Signal Model

For the signal model, we consider the time-varying channel impulse response [6]

$$h_p(t, d_\tau) = \frac{1}{\sqrt{(4\pi Dt)^3}} e^{-\frac{d_\tau^2}{4Dt}}, \tag{5}$$

where d_τ is the time-varying distance between leader and follower at the time of emission for bit j.

Then, a suitable threshold, to reduce the impact of ISI, can be chosen as [21]

$$N_h = \frac{M_0}{\ln\left(1 + \frac{M_0}{\sum_{j=1}^{L_c} \frac{M_j}{2} + \lambda_0 T_b}\right)}. \tag{6}$$

where we define

$$M_j = N_{T_x} V_{R_x} h_p(T_d + (j-1)T_b, d_\tau), \tag{7}$$

which accounts for ISI, and λ_0 is the background noise per unit time [21].

Assuming the reception process is also noisy, the received signal for bit j can be described probabilistically by [21]

$$N_{R_x}(t_j) \sim \mathcal{P}(b_j M_0 + n_{\text{ISI}}(t_j) + \lambda_0 T_b), \tag{8}$$

where $\mathcal{P}(\cdot)$ denotes the Poisson distribution, b_j is the j-th transmitted bit and the term $n_{\text{ISI}}(t_p)$ accounts for the ISI according to

$$n_{\text{ISI}}(t_j) = \sum_{j=1}^{L_c} b_{L_c - j} N_{T_x} V_{R_x} h(t_j + j T_b, d_\tau), \tag{9}$$

where L_c is the channel length.

III. SYSTEM ANALYSIS

In this section, we analyze the distance between leader and follower over time. As a reference, we note that for stationary nodes, without coding, the bit error rate is given in [21]. However, for the leader-follower scenario considered here, estimation errors lead to random changes in the distance between the nodes, which in turn impacts the error rate in a complicated manner due to the time-variant channel and the coding.

At a given time instant, when no errors are produced, the distance between the transmitter and the receiver is equal to the initial distance x_0. When only one error is produced ($k_n = 1$), then we add to the previous distance an additional quantity $\Delta_\epsilon \leq 2\Delta$ to account for errors that will always increase the distance between both nodes (as a worst-case scenario). Considering the randomness of the leader node position, an upper bound in the x-direction can be given by

$$\Delta x_n \leq \Delta x_n^{(u)} = \Delta x_0 + k_n \cdot 2\Delta, \tag{10}$$

where n is the time-index to indicate the sample time as $t_n = n\Delta t$, and x_0 is the initial distance in x-axis direction. Here, x_0 is the initial separation and Δ_ϵ is the increase in distance in case of an error. The variable $k_n \in \mathbb{N}$ will assess the total number of errors which occurred until time instant n.

Despite the interdependence of distance between leader and follower and error probability over time, in general, for each time instant n an error can be modeled as a Bernoulli random variable [22] with a time-dependent occurrence probability $p_e(t_i)$. Then, k_n will be the accumulated value of n Bernoulli random variables with different occurrence probability each. In general, the error events will not be independent. Nevertheless, we assume that the accumulated number of errors can be modeled as a Poisson-Binomial random variable with the occurrence probabilities $p_e(t_i)$.

For ease of analysis and assuming a sufficiently large number of attempts, we will further approximate the distribution of k_n by a normal distribution as

$$k_n \sim \mathcal{N}\left(\sum_{i=1}^{n} p_e(t_i), \sum_{i=1}^{n} p_e(t_i)(1 - p_e(t_i))\right). \tag{11}$$

In summary, using this Gaussian approximation for k_n, the considered upper bound for Δx_n in (10) comprises the sum of a deterministic value x_0 and a normal random variable scaled by 2Δ. Hence, under these conditions, the considered upper bound will also be normally distributed as

$$x_n^{(u)} \sim \mathcal{N}\left(\mu_{x_n^{(u)}}, \sigma_{x_n^{(u)}}^2\right), \tag{12}$$

with mean and variance

$$\mu_{x_n^{(u)}} = 2\Delta \sum_{i=1}^{n} p_e(t_i) + x_0, \tag{13}$$

$$\sigma_{x_n^{(u)}}^2 = 4\Delta^2 \sum_{i=1}^{n} p_e(t_i)(1 - p_e(t_i)). \tag{14}$$

The same argument can be analogously repeated for the other two spatial directions y and z, replacing x_0 with y_0 and z_0, respectively. Hence, the corresponding upper bounds for Δy and Δz will also be normally distributed. Finally, considering that $d = \sqrt{(\Delta x)^2 + (\Delta y)^2 + (\Delta z)^2}$, we can obtain an approximate upper bound for the distance between leader and follower as the square-root of the sum of squared normal random variables, which in turn yields the non-central Chi distribution with 3 degrees of freedom as [23]

$$d_n^{(u)} \sim \chi\left(3, \lambda_n\right), \tag{15}$$

where

$$\lambda_n = \frac{\mu^2_{x_n^{(u)}} + \mu^2_{y_n^{(u)}} + \mu^2_{z_n^{(u)}}}{\sigma_n^2}, \tag{16}$$

and $\sigma_n^2 = \sigma^2_{x_n^{(u)}}$ as given in (14).

Based on the derived probability density function in (15), we can analyze the average behavior of the upper bound with time when considering the average value of the non-central Chi distribution as [23]

$$\overline{d}_n^{(u)} = \mu_{d_n^{(u)}} = \sqrt{\frac{\pi \sigma_n^2}{2}} L_{1/2}^{(1/2)}\left(-\frac{\lambda_n^2}{2}\right), \tag{17}$$

where $L^{(\cdot)}(\cdot)$ is the Laguerre function.

By the relation in (17), the average distance between both nodes will be time dependent through parameter λ_n given in (16). The time dependence of $\overline{d}_n^{(u)}$ is ultimately caused by the time dependence of the bit error probability $p_e(t_n)$, which is unknown in this scenario.

Since $p_e(t_i)$ cannot be specified analytically due to the interdependence with the distance and the applied coding, in the following we will assume several general parametric descriptions of $p_e(t_i)$. Then, we numerically evaluate the corresponding impact on the derived upper bound in Section IV.

IV. NUMERICAL RESULTS

In this section, we validate our theoretical upper bound on the leader-follower distance in (17) by comparing it with simulation results. Simulation generally follows the description in Section II and is implemented by simulating the discrete random walk of leader and follower, i.e., the random distance between leader and follower is simulated directly while the number of received molecules at the follower is simulated by a Poisson random number generator. As parameters, we choose $L_c = 1$ for evaluating the ISI in (9) [24], a background noise of $\lambda_0 = 100\,\mathrm{s}^{-1}$, an initial distance of $10^{-7}\,\mathrm{m}$, and discrete time steps of size $\Delta t = 1\,\mathrm{ms}$.

In Fig. 3, we show the distance between leader and follower over time for 1000 realizations (d_τ) of the random walk of the leader. Interestingly, for the simulation results, the average distance ($\overline{d}_\tau$ sim.) is increasing in a linear fashion over time. We note that the density of realizations below the average is larger than above, i.e., visually the curve for $\overline{d}_\tau$ is much smaller than the realization with the largest overall distance. The theoretical upper bound in (17) is also depicted in Fig. 3 by assuming three different behaviors for
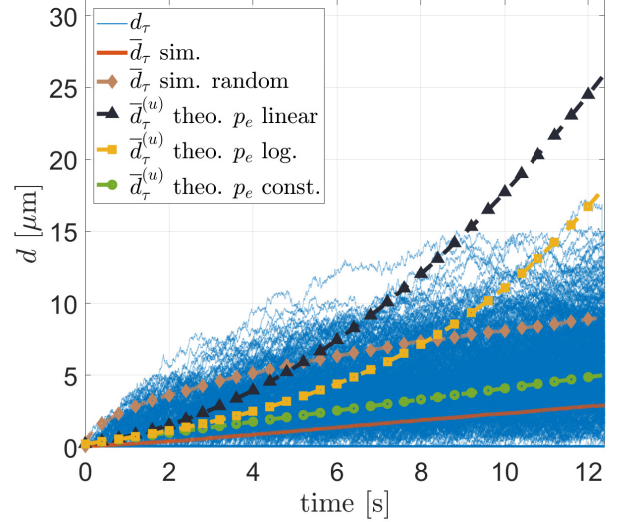

Fig. 3. Varying distance between the leader and follower nodes.

the error probability regarding their dependency on time. For normalizing these functions, by simulation, we obtain an initial error rate of 10^{-1}, which in the following is denoted by p_{e_0}. On the one hand, when considering a linear relation with time (order 1) as $p_e(t_n) = p_{e_0} \cdot (n10^{-3} + 1)$, visually, a better fit with the average simulated curve is obtained for small times compared to large times ($\overline{d}_\tau^{(u)}$ theo. p_e linear). On the other hand, when modeling the time dependence of the underlying error probability as a logarithmic function by $p_e(t_n) = p_{e_0} \cdot (1 + \ln(1 + n10^{-3}))$, then we obtain an even better fit, especially for small times ($\overline{d}_\tau^{(u)}$ theo. p_e log.). Finally, when assuming a constant behavior via $p_e(t_n) = p_{e_0}$, which represents a steady behavior, then we obtain the tightest upper bound for the given simulation results ($\overline{d}_\tau^{(u)}$ theo. p_e const.). As a reference, we also show the distance over time for the scenario when the leader and follower move randomly and independently from each other. In this case, leader and follower quickly spread and the average simulated curve is significantly smaller than this benchmark, highlighting the effectiveness of the proposed communication scheme. The same conclusion also holds for the theoretical upper bound in the case of a constant error rate behavior. Considering the theoretical results depicted in Fig. 3, the best fit with the simulated results is obtained when $p_e(t_n)$ is assumed to be constant with time. Hence, we will use this upper bound for the following analysis.

In Fig. 4, we study the impact of different diffusion coefficients for the signaling particles. To this end, we consider the ratio D/D_{T_x} as a parameter, i.e., the relative diffusivity of the signaling molecules compared to the leader diffusivity. As expected, the larger the ratio the better the tracking performance. That is, the movement of the leader node will be slow compared to the signaling molecules, which in turn implies smaller jumps per time step and thus a reduced number
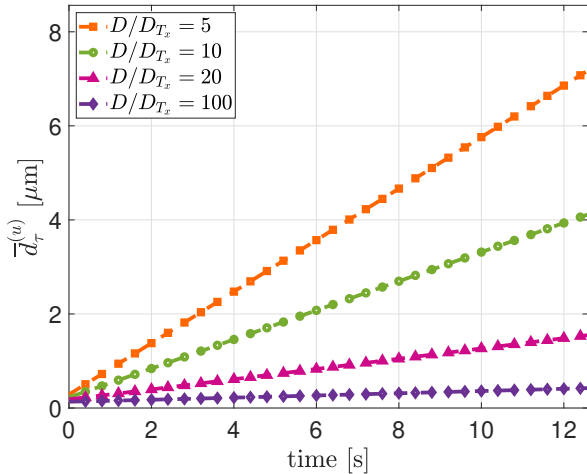
Fig. 4. Varying distance for different values of the diffusion coefficient.

of errors benefiting the tracking performance. In particular, for diffusion coefficient ratios larger than 20, the slope of the average upper bound will be small, which indicates that the distance between both nodes will behave quasi-stationary. This result can also be interpreted as follows. According to the Einstein relation [6], the diffusion coefficient is inversely proportional to the molecule size. Hence, the ratio D/D_{T_x} can also be interpreted as the relative size of the leader compared to the signaling molecules. Here, if the leader is 100 times larger than the signaling molecules, the distance between leader and follower will be almost constant.

We note that although the results provided here are based on a particular mobility model of the leader, the derived upper bound in (17) is generally applicable since it does not directly depend on the chosen mobility model. A given mobility model will correspondingly only need to be accounted for in the assumed model for $p_e(t)$.

V. Conclusion

This paper provides a first approach to theoretically analyze the tracking of a leader node by a follower node in a mobile molecular communication scenario. A simple communication scheme based on transmitting position increments from leader to follower has been devised and its effectiveness is demonstrated compared to a benchmark of uncoordinated movement of leader and follower. Moreover, a closed-form expression for an upper bound on the distance between leader and follower is derived and validated by simulation results. The presented approach allows predicting the conditions necessary for a follower to reliably track a leader node, which is crucial in mobile nanonetworks comprising multiple follower nodes.

Our research can be further elaborated in a variety of directions to address more realistic scenarios and improved designs. For instance, the limited resources of the leader node to synthesize molecules, the use of relay nodes to increase the network size, the analysis of different communication strategies including the impact of the modulation technique, the application of different analytical tools such as the age of information metric to study delay and error rate jointly, the study of the nanonetwork formation in different topologies with multiple leader nodes, or the impact of particular nanosensor mobility models. Also, studying further channel effects such as the impact of turbulence, sedimentation, and drift, or the use of more elaborated mathematical tools to account for unknown system parameters such as ordered weighted average operators.

References

[1] W. Haselmayr, A. Springer, G. Fischer, C. Alexiou, H. Boche, P. A. Hoeher, F. Dressler, and R. Schober, "Integration of Molecular Communications into Future Generation Wireless Networks," in *1st 6G Wireless Summit*. Levi, Finland: IEEE, Mar. 2019.

[2] T. Nakano, Y. Okaie, S. Kobayashi, T. Hara, Y. Hiraoka, and T. Haraguchi, "Methods and Applications of Mobile Molecular Communication," *Proceedings of the IEEE*, vol. 107, no. 7, pp. 1442–1456, Jul. 2019.

[3] C. A. Soldner, E. Socher, V. Jamali, W. Wicke, A. Ahmadzadeh, H.-G. Breitinger, A. Burkovski, K. Castiglione, R. Schober, and H. Sticht, "A Survey of Biological Building Blocks for Synthetic Molecular Communication Systems," *IEEE Communications Surveys & Tutorials*, vol. 22, no. 4, pp. 2765–2800, 2020.

[4] Y. Lu, R. Ni, and Q. Zhu, "Wireless Communication in Nanonetworks: Current Status, Prospect and Challenges," *IEEE Transactions on Molecular, Biological and Multi-Scale Communications*, vol. 6, no. 2, pp. 71–80, Nov. 2020.

[5] Y. Okaie, T. Nakano, T. Hara, T. Obuchi, K. Hosoda, Y. Hiraoka, and S. Nishio, "Cooperative Target Tracking by a Mobile Bionanosensor Network," *IEEE Transactions on NanoBioscience*, vol. 13, no. 3, pp. 267–277, Sep. 2014.

[6] V. Jamali, A. Ahmadzadeh, W. Wicke, A. Noel, and R. Schober, "Channel Modeling for Diffusive Molecular Communication—A Tutorial Review," *Proceedings of the IEEE*, vol. 107, no. 7, pp. 1256–1301, Jul. 2019.

[7] S. Huang, L. Lin, H. Yan, J. Xu, and F. Liu, "Mean and Variance of Received Signal in Diffusion-Based Mobile Molecular Communication," in *IEEE Global Communications Conference (GLOBECOM 2018)*. Abu Dhabi, United Arab Emirates: IEEE, Dec. 2018.

[8] G. Chang, L. Lin, and H. Yan, "Adaptive Detection and ISI Mitigation for Mobile Molecular Communication," *IEEE Transactions on NanoBioscience*, vol. 17, no. 1, pp. 21–35, Jan. 2018.

[9] A. Ahmadzadeh, V. Jamali, and R. Schober, "Stochastic Channel Modeling for Diffusive Mobile Molecular Communication Systems," *IEEE Transactions on Communications*, pp. 6205 – 6220, Dec. 2018.

[10] L. Lin, Q. Wu, F. Liu, and H. Yan, "Mutual Information and Maximum Achievable Rate for Mobile Molecular Communication Systems," *IEEE Transactions on NanoBioscience*, vol. 17, no. 4, pp. 507–517, Oct. 2018.

[11] A. K. Shrivastava, D. Das, R. Mahapatra, and S. P. Mohanty, "dMole: A Novel Transreceiver for Mobile Molecular Communication Using Robust Differential Detection Techniques," *IEEE Transactions on NanoBioscience*, vol. 19, no. 4, pp. 609–621, Oct. 2020.

[12] J. Wang, X. Liu, M. Peng, and M. Daneshmand, "Performance Analysis of D-MoSK Modulation in Mobile Diffusive-Drift Molecular Communications," *IEEE Internet of Things Journal*, vol. 7, no. 11, pp. 11 318–11 326, Nov. 2020.

[13] Y. Okaie and T. Nakano, "Mobile Molecular Communication Through Multiple Measurements of the Concentration of Molecules," *IEEE Access*, vol. 8, pp. 179 606–179 615, Jan. 2020.

[14] X. Mu, H. Yan, B. Li, M. Liu, R. Zheng, Y. Li, and L. Lin, "Low-Complexity Adaptive Signal Detection for Mobile Molecular Communication," *IEEE Transactions on NanoBioscience*, vol. 19, no. 2, pp. 237–248, Apr. 2020.

[15] Y. Okaie, S. Ishiyama, and T. Hara, "Leader-Follower-Amplifier Based Mobile Molecular Communication Systems for Cooperative Drug Delivery," in *IEEE Global Communications Conference (GLOBECOM 2018)*. Abu Dhabi, United Arab Emirates: IEEE, Dec. 2018.

[16] T. Nakano, Y. Okaie, S. Kobayashi, T. Koujin, C.-H. Chan, Y.-H. Hsu, T. Obuchi, T. Hara, Y. Hiraoka, and T. Haraguchi, "Performance Evaluation of Leader-Follower-Based Mobile Molecular Communication Networks for Target Detection Applications," *IEEE Transactions on Communications*, vol. 65, no. 2, pp. 663–676, Feb. 2017.

[17] Y. Okaie, T. Nakano, T. Obuchi, S. Ishiyama, and T. Hard, "Molecule gradient formation by mobile bio-nanomachines," in *International Symposium on Intelligent Signal Processing and Communication Systems (ISPACS 2017)*. Xiamen, China: IEEE, Nov. 2017.

[18] W.-K. Hsu, X. Lin, and M. R. Bell, "Deep-Target Delivery of Nanosensors with Bacteria-Inspired Coordination," in *IEEE Global Communications Conference (GLOBECOM 2017)*. Singapore, Singapore: IEEE, Dec. 2017.

[19] M. S. Kuran, H. B. Yilmaz, I. Demirkol, N. Farsad, and A. Goldsmith, "A Survey on Modulation Techniques in Molecular Communication via Diffusion," *IEEE Communications Surveys & Tutorials*, vol. 23, no. 1, pp. 7–28, Jan. 2021.

[20] A. B. Carlson, *Communication Systems: An introduction to signals and noise in electric communications*, 5th ed. Boston, Mass.: McGraw Hill Higher Education, 2009.

[21] X. Qian, M. D. Renzo, and A. W. Eckford, "Molecular Communications: Model-Based and Data-Driven Receiver Design and Optimization," *IEEE Access*, vol. 7, pp. 53 555–53 565, Jan. 2019.

[22] Y. H. Wang, "On the Number of Successes in Independent Trials," *Statistica Sinica*, vol. 3, no. 2, pp. 295–312, 1993.

[23] M. Krishnan, "The Noncentral Bivariate Chi Distribution," *SIAM Review*, vol. 9, no. 4, pp. 708–714, Oct. 1967.

[24] A. Aijaz and A.-H. Aghvami, "Error Performance of Diffusion-Based Molecular Communication Using Pulse-Based Modulation," *IEEE Transactions on NanoBioscience*, vol. 14, no. 1, pp. 146–151, Jan. 2015.